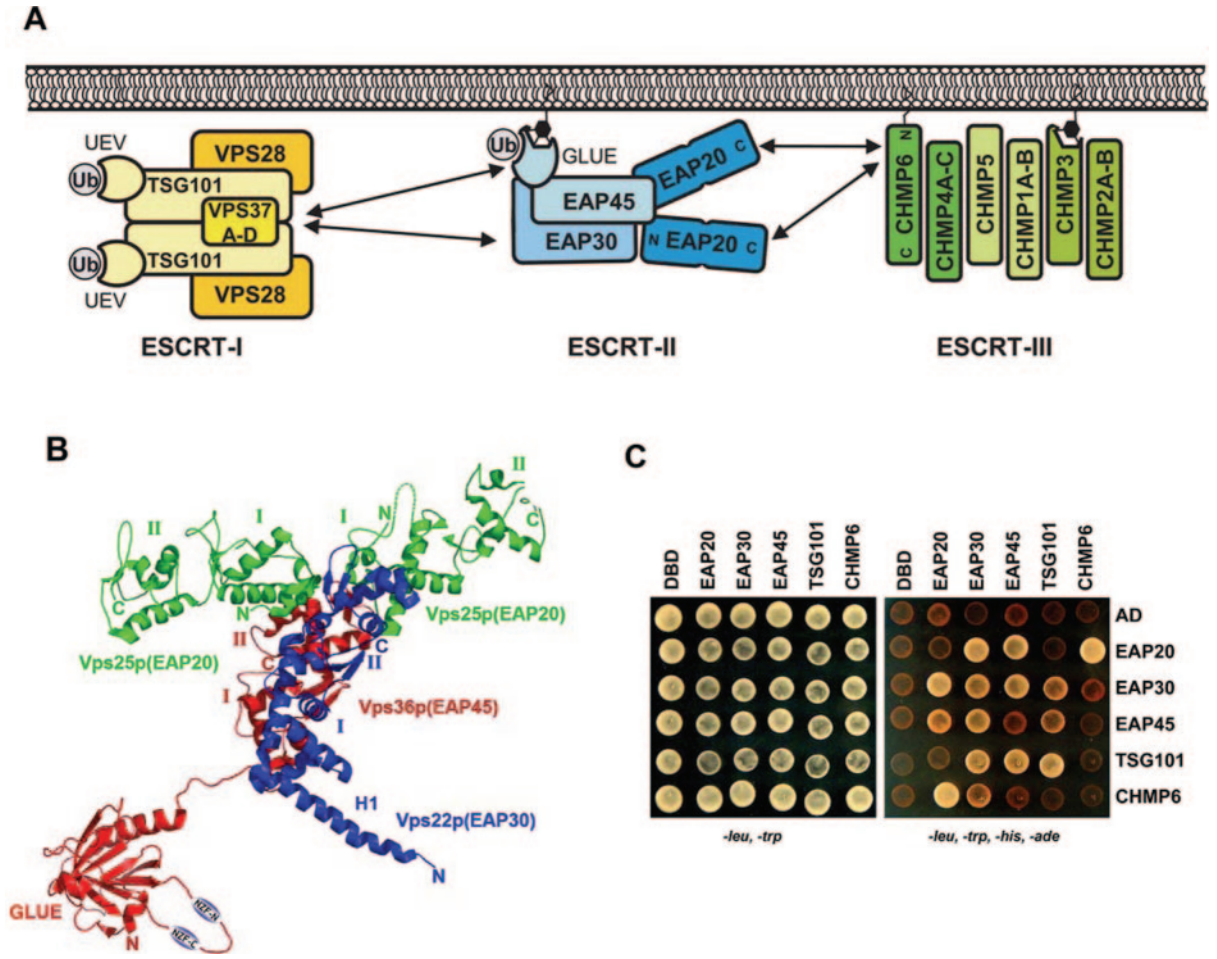

FIG. 1. ESCRT-II structure and interactions. (A) Schematic model summarizing the protein interactions of the human ESCRT-II complex (see the text for details). Note that the stoichiometries and compositions of the ESCRT-I and ESCRT-III complexes have not yet been defined unambiguously. The complexes are therefore simply shown with all possible subunits. (B) Three-dimensional structure of the yeast ESCRT-II complex. The structure of the ESCRT-II core was determined by X-ray crystallography (30, 74). The N-terminal region of Vps36 (EAP45) (shown schematically) has not yet been determined but contains two NZF domains (1) embedded within a GLUE domain (67). The structural elements/domains correspond approximately to the following residues (human homologs are in parentheses): for Vps36p (EAP45), GLUE domain, 1 to 285 (1 to 135); NZF-1, 177 to 205; NZF-2, 242 to 259 (neither NZF motif is present in EAP45); linker domain, 286 to 404 (136 to 238); WH-1, 405 to 491 (239 to 316); and WH-2, 492 to 566 (317 to 386); for Vps22p (EAP30), helix 1 (H1), 1 to 51 (1 to 55); WH-1, 90 to 165 (95 to 176); and WH-2, 166 to 233 (177 to 258); for Vps25p (EAP20), WH-1, 19 to 127 (22 to 103), and WH-2, 128 to 200 (104 to 176). (C) Summary of the positive yeast two-hybrid interactions between ESCRT-II proteins and all known human class E proteins. The right array shows doubly transformed yeast replica plated on minus Leu, minus Trp, minus His, minus Ade selection media, where successful growth represents a positive protein interaction. The left array shows replica-plated yeast on minus Leu, minus Trp media (a control for equivalent transformation and yeast growth). The indicated constructs were fused to DBDs (rows) or ADs (columns). Unfused DBD and AD constructs are shown as negative controls. Note that the interaction between DBD-EAP30 and AD-CHMP6 was judged to be negative because it was very weak and was not detected in the reciprocal direction. Analogous data were summarized previously in reference 83.

lated as a stable, soluble complex composed of three proteins that share 19 to 36% pairwise identity with their *S. cerevisiae* homologs (excluding the N-terminal region of Vps36p/EAP45) (37, 61). We have therefore used the crystal structure of the *S. cerevisiae* ESCRT-II core as a working model for the human ESCRT-II complex (Fig. 1B) (see Materials and Methods). Mammalian ESCRT-II functions are less well studied than those of the yeast complex, but the mammalian EAP20 and EAP45 proteins do colocalize with ESCRT-III components and with ubiquitylated proteins on endosomal membranes (67, 88). Like their yeast counterparts, EAP20 can bind the ESCRT-III protein, CHMP6 (46, 83, 88), and the N-terminal GLUE domain of murine EAP45 was recently shown to bind ubiquitin (67). These observations all support the idea that the mammalian and *S. cerevisiae* ESCRT-II complexes are functional homologs. Nevertheless, there must also be important differences between human and yeast ESCRT-II proteins. For example, the mammalian complex lacks both NZF domains and therefore must interact differently with both ESCRT-I and ubiquitin. Moreover, ESCRT-II and CHMP6 overexpression does not inhibit HIV type 1 (HIV-1) budding (46), and it was recently reported that ESCRT-II is not required for lysosomal degradation of major histocompatibility complex I (MHC-I) or epidermal growth factor receptor (EGFR), indicating that the